

Thermal properties and processability of modified poly(L-lactide): the role of phenylacetic acid hydrazide derivative

Hao Huang¹, Yanhua Cai^{1, *} (ORCID ID: 0000-0002-1390-3722), Lisha Zhao¹

DOI: <https://doi.org/10.14314/polimery.2022.9.3>

Abstract: The influence of phenylacetic acid hydrazide (NAPAH) derivative content, melt temperature (170–200°C) and cooling rate (1–20°C/min) on poly(L-lactide) (PLLA) nucleation were investigated. Increasing the content of NAPAH (0.5–3.0 wt.%) had a positive effect on PLLA crystallization, while an increase in the cooling rate and heating temperature had a negative effect. In the case of isothermal crystallization carried out for a long time (180 min), the melting process depended only on the crystallization temperature. NAPAH also influenced the cold crystallization temperature, reduced thermal stability and improved PLLA processability (MFR).

Keywords: poly(L-lactide), phenylacetic acid hydrazide, naphthalenedicarboxylic acid, organic nucleating agent, thermal properties.

Właściwości termiczne i przetwórcze modyfikowanego poli(L-laktydu): rola pochodnej hydrazynu kwasu fenyllooctowego

Abstrakt: Zbadano wpływ zawartości pochodnej hydrazynu kwasu fenyllooctowego (NAPAH), temperatury stopu (170–200°C) i szybkości chłodzenia (1–20°C/min) na nukleację poli(L-laktydu) (PLLA). Zwiększenie zawartości NAPAH (0,5–3,0% mas.) miało pozytywny wpływ na krystalizację PLLA, natomiast wzrost szybkości chłodzenia i temperatury ogrzewania negatywny. W przypadku krystalizacji izotermicznej prowadzonej przez długi czas (180 min), proces topnienia zależał tylko od temperatury krystalizacji. NAPAH wpływał również na temperaturę zimnej krystalizacji, zmniejszał stabilność termiczną i poprawiał właściwości przetwórcze PLLA (MFR).

Słowa kluczowe: poli(L-laktyd), hydrazyn kwasu fenyllooctowego, kwas naftalenodikarboksylowy, organiczny środek nukleujący, właściwości termiczne.

With the implementation of global plastic ban, poly(L-lactide) (PLLA) as a leading product of biodegradable plastics has obtained increasing attention due to its excellent properties, such as excellent biocompatibility and controllable biodegradability [1–3], competitive stiffness and tensile strength [4, 5], and originating from renewable resource [7]. It is also harmless to humans and environmentally friendly [6], and originating from renewable resource [7]. Therefore it has been expanded to more fields to replace the traditional petro-based resins, especially in packaging materials [8–10], bone regeneration [11–13], nonwovens [14–16] and agriculture [17–19].

However, the practical applications of PLLA in field of industrial production and daily life are much less than expected because of its some inherent disadvantages

including low melt strength, poor heat resistance, and slow crystallization rate [20, 21]. Among these disadvantages, slow crystallization rate is thought to be the most significant disadvantage of PLLA in comparison to the general purpose plastics like PP and PE, because the crystallization rate not only determines PLLA's crystallinity and heat resistance, but also affects PLLA's molding cycle during actual manufacturing. Therefore, improving the crystallization of PLLA is still a huge challenge. Tremendous efforts have been carried out to regulate the crystallization rate of PLLA, mainly including four typical approaches. They added nucleating agent or plasticizer, minimizing the amount of D-lactide isomers and adjusting the molding conditions [22]. Compared to the nucleating agent, the other three ways exhibit more obvious disadvantages in usage. For instance, the plasticizer tends to spill over PLLA matrix leading to non-persistent characteristic for promoting crystallization while adjusting the molding conditions results in the high energy-consumption. In contrast, a nucleating agent exhibits powerful

¹ Chongqing University of Arts and Sciences, College of Chemistry and Environmental Engineering, College of Pharmaceutical Sciences, Chongqing-402160, P.R. China.

* Author for correspondence: mci651@163.com

advantages such as low dosage, high nucleation efficiency and simple operation, therefore it seems almost feasible for industrial accelerating crystallization to adding a nucleating agent in PLLA resin. In the early stages, it is popular to accelerate crystallization rate of PLLA by melt blending with inorganic nucleating agents including talc [23], organically modified montmorillonite [24], nano-sized CaCO_3 [25], carbon black [26], etc. Recently, organic low molecular weight compounds have been drawing much attention, since they exhibit some special features in compatibility with PLLA, molecular structure regulation and nucleation efficiency. As a result, a large number of organic low molecular weight compounds were developed as organic nucleating agents to modify PLLA, including the relatively earlier hydrazide compounds [27, 28], oxalamide compounds [29, 30], humic acid derivatives [31, 32], piperonylic acid derivatives [33, 34], 1H-benzotriazole compounds [35, 36], etc. Through molecular structure analysis, it is found that the most of these organic nucleating agents contain active groups (like N-H or O-H) and rigid structures (like benzene or cyclopentane), indicating that to some extent these key groups or structures play an important role in accelerating nucleation and crystallization of PLLA. Of course, these related speculations needs to be confirmed by developing more organic nucleating agents and estimating their nucleation effects on PLLA's crystallization. On the basis of the aforementioned reason, in this study, amide and naphthalene were introduced into developing strategy of organic nucleating agent to obtain a new nucleating agent named *N, N'*-bis(phenylacetyl) 1, 4-naphthalenedicarboxylic acid dihydrazide (NAPAH), and the related properties of PLLA with different NAPAH content were investigated in terms of crystallization, melting behaviors, thermal stability and processability (MFR). Moreover, the aim of the research was to evaluate the influence of active groups and rigid structures on PLLA nucleation and to determine the structure-nucleating agent activity relationship.

EXPERIMENTAL PART

Materials and reagents

A semi-crystalline PLLA (4032D) was manufactured by Nature Works. The nucleating agent NAPAH was synthesized in our laboratory (The synthesis process was exhibited in the upcoming synthesis of NAPAH), and all used analytical pure reagents, including 1, 4-naphthalenedicarboxylic acid, phenylacetic hydrazide, thionyl chloride, pyridine and *N, N*-dimethylformamide, were purchased from Chongqing Huanwei Chemical Company to direct use without further purification.

Synthesis of NAPAH

The chemical structural formula of NAPAH was shown in Figure.1. Two step reactions were used to synthesize NAPAH as reported BAAD in our research group [37],

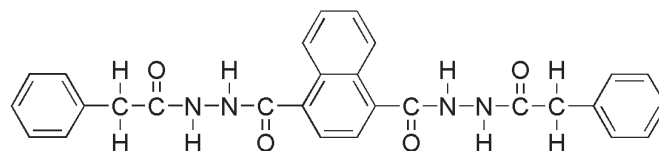


Fig. 1. Chemical formula of NAPAH

the first step reaction was acylation of 1, 4-naphthalenedicarboxylic acid to obtain 1, 4-naphthalenedicarboxylic acid dichloride; the second step reaction was amination reaction of phenylacetic hydrazide with 1, 4-naphthalenedicarboxylic acid dichloride. Finally, the white product NAPAH was thoroughly dried at the temperature of 35°C under vacuum for usage. FT-IR (KBr) ν : 3180.9, 3027.7, 1664.5.1, 1598.4, 1514.0, 1480.9, 1453.6, 1425.3, 1388.1, 1291.2, 1249.8, 1173.8, 1151.6, 853.1, 722.5, 695.2 cm^{-1} ; ^1H NMR (400 Hz) δ : ppm; 10.46 (s, 1H, NH), 10.33 (s, 1H, NH), 8.20~8.38 (m, 1H, Py), 7.85~7.96 (d, 2H, Py), 7.24~7.66 (m, 5H, Ar), 3.59 (s, 2H, CH_2).

PLLA/NAPAH preparation

Before melt-mixing, the PLLA and various NAPAH content were first mixed at room temperature, and the mixture was dried at the temperature of 35°C under vacuum for 24 h to remove moisture. And then the blend of PLLA with NAPAH was melted on a torque rheometer at the temperature of 190°C for 17 min (32 rpm for 7 min and 64 rpm for 10 min). After that, the mixture was further processed by hot-pressing and cool-pressing to obtain the final sample. In this study, the NAPAH content was varied as 0, 0.5, 1, 2 and 3 wt%, and the corresponding samples were labeled as PLLA, PLLA/0.5%NAPAH, PLLA/1%NAPAH, PLLA/2%NAPAH and PLLA/3%NAPAH, respectively.

Methods

The molecular structure characterization of NAPAH was determined by IS50 FT-IR (Thermo Fisher Scientific) and AVANCE 400MHz ^1H NMR (Bruker). The FT-IR characterization adopted KBr pressed-disk technique, and the test wave number was from 4000 cm^{-1} to 400 cm^{-1} . As a solvent of ^1H NMR characterization, deuteration dimethyl sulfoxide was used. The studies on the crystallization and melt of the virgin PLLA and four PLLA/NAPAH samples were performed by Q2000 DSC (TA Instruments) with nitrogen flow of 50 ml/min, and before testing, the temperature and heat flow calibration needed to be completed, as well as the thermal history needed to be eliminated to ensure the test at the same level. The thermal decomposition processes of NAPAH, the virgin PLLA and four PLLA/NAPAH samples were recorded by Q500 TGA (TA Instruments) produced by TA instruments, and the testing temperature ranged from 50 to 650°C at a heating rate of 5°C/min in air; however, for the thermal decomposition of NAPAH, two other heating rates

of 1°C/min and 10°C/min were added to investigate the influence of heating rate on the thermal decomposition behavior of NAPAHA. The melt flow rate was used to characterize PLLA processability, and the melt flow rate was obtained by RTSL-400B melt index instrument (Beijing Guance Instrument) with testing temperature of 180°C.

RESULTS AND DISCUSSION

Thermal decomposition of NAPAHA

The excellent thermal stability is the basic requirement of a nucleating agent for PLLA, because a nucleating agent should not be decomposed during melting blend. Figure 2 shows the thermal decomposition TGA curves of the NAPAHA at different heating rates in air. It can be clearly observed from TGA curves that NAPAHA cannot decompose in the melting blend temperature region of 170°C to 200°C, indicating that NAPAHA can be used as additive for PLLA in terms of thermal stability. For the thermal decomposition process of NAPAHA, there are two main weight loss stages in TGA curve, and the first main weight loss stage occurs in the temperature region of 300°C to 400°C, exhibiting more than 60% weight loss; and the second main stage has less than 30% weight loss. Additionally, with increasing of heating rate, the TGA curve shifts toward the higher temperature side and the onset thermal decomposition temperature also increases, resulting from the thermal inertia.

Crystallization behavior of PLLA/NAPAHA

For semi-crystalline polyester, many physical properties including mechanical properties, heat resistance and optical performance depend on the crystallization behavior of polyester. Thus, in this work, the cooling processes comparison of the virgin PLLA and PLLA/NAPAHA samples from the melt of 190°C was first performed by DSC. As seen in Fig. 3, upon the cooling at 1°C/min, the crystallization of the virgin PLLA almost cannot occur in

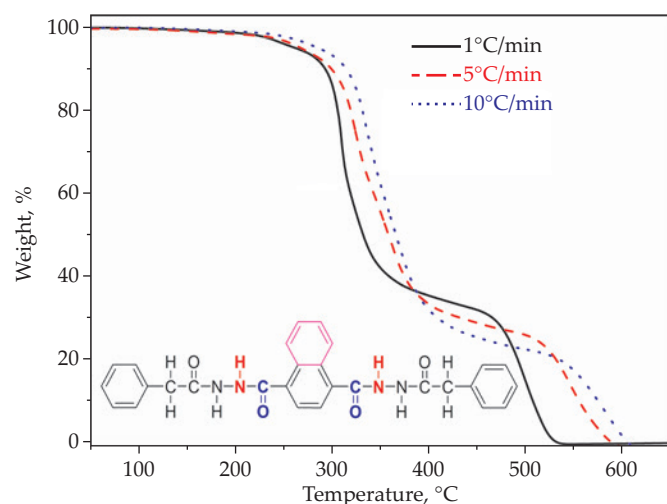


Fig. 2. TGA curves of the NAPAHA

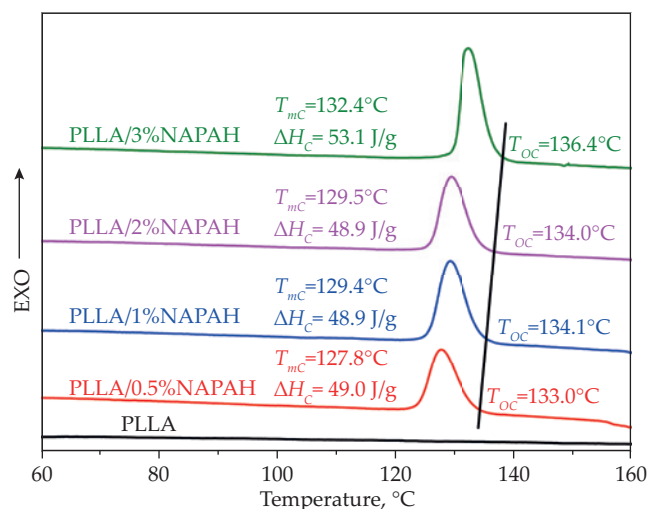


Fig. 3. Melting cooling processes of the virgin PLLA and PLLA/NAPAHA from the melt of 190°C at a rate of 1°C/min

cooling, which was thought to be because of two probable reasons. First reason is that it is difficult for virgin PLLA to form a nucleus in the high temperature region, resulting in a slow nucleation rate and second reason is that the motility of PLLA molecular chain is very poor in the low temperature region, resulting in slow crystal growth rate. In contrast, the existence of NAPAHA makes the PLLA to form remarkable and sharp melt-crystallization peaks in DSC curves as shown in Fig. 3, indicating the powerful enhancing crystallization role of NAPAHA for PLLA, because NAPAHA as external additive can provide a larger amount of heterogeneous nucleation sites in PLLA matrix, which shortens the crystallization induction time of PLLA and causes the crystallization to occur in higher temperature region, this result is also proved by the effect of NAPAHA concentration on the onset crystallization temperature (T_{oc}), that is, with increasing of NAPAHA concentration from 0.5 to 3 wt%, the T_{oc} increases from 133.0°C to 136.4°C. PLLA/NAPAHA sample not only has a fast nucleation rate, but also PLLA molecular segment possesses excellent motility in preliminary stage of cooling, which ensures that the PLLA crystal can be effectively grown in cooling. Usually, the smaller the difference (ΔT) between the T_{oc} and melt-crystallization peak temperature (T_{mc}) is, the faster the crystallization rate is, as well as that the bigger nucleating effect on PLLA crystallization is. It is evident from Fig. 3 that that PLLA/3%NAPAHA exhibits the minimum ΔT value of 4°C and the largest melt-crystallization enthalpy (ΔH_c) of 56.1 J/g, indicating that, with the addition of 3 wt% NAPAHA, the modified PLLA has the most powerful crystallization ability. Additionally, when compared with some systems like PLLA/CB [38] and PLLA/BAS [39], PLLA/3%NAPAHA has higher T_{oc} and ΔH_c in the same testing level, this result shows that NAPAHA has better acceleration effectiveness on the melt-crystallization of PLLA.

Upon the melt of 190 °C, the melt-crystallization behaviors of PLLA/NAPAHA at various cooling rates from 5 to

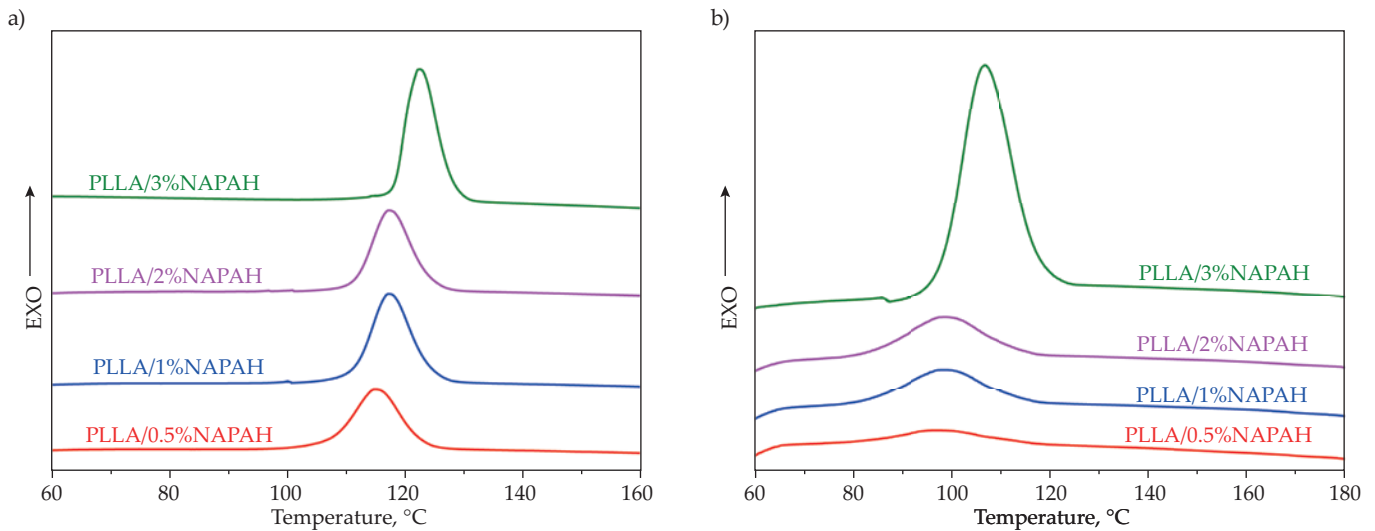


Fig. 4. Melting-cooling processes of PLLA/NAPAH samples from the melt of 190°C at various rates: a) 5°C/min, b) 20°C/min

20°C/min were investigated by DSC (See Fig. 4). When the cooling rate is 5°C/min, the crystallization peak of a given PLLA/NAPAH sample appears in the relatively low temperature region comparing with the relative peak in cooling at 1°C/min. Moreover, the peak shape of crystallization evidently become wider and the ΔT also becomes larger, showing that the crystallization ability of NAPAH-nucleated PLLA is weakened, the probable reason depends on the effect of the cooling rate on the crystal growth, a higher cooling rate have a time inhibition for the regular arrangement of PLLA chain segment. The similar results can be found in literatures [38, 40, 41]. When the cooling rate is increased to 20°C/min, the crystallization ability is further weakened, even the melt-crystallization peak of PLLA/0.5%NAPAH almost cannot be observed in DSC curve.

However, an increase of heating rate makes the cold-crystallization peak move toward the high-temperature side because of the thermal inertia; and the cold-crystallization process is completed in a wider temperature range as seen in Fig. 5. This effect is reflected by the subsequent melting behavior of cold-crystallization. The melting pro-

cess appears in the higher temperature region when the sharper cold-crystallization peak appears, because the sharper cold-crystallization peak means more consistent crystal perfection. In addition, it is noted that the cold-crystallization of PLLA containing a larger amount of NAPAH appears in heating earlier, and the cold-crystallization temperature of PLLA shifts to a maximum value with the lowest NAPAH content of 0.5 wt%, as well as the cold-crystallization peak becomes flatter as NAPAH concentration increases. These results suggest that NAPAH inhibits the cold-crystallization process of PLLA.

For melt-crystallization process, some literatures [42, 43] had reported the significant influences of the melt temperature on the modified PLLA crystallization processes, and the relative studies are very important to reveal in-depth the role of additive in PLLA resin and determine the processing conditions. Here, the effects of the other two melt temperatures (170 and 200°C) of the NAPAH-nucleated PLLA crystallization processes were estimated by DSC with a cooling rate of 1°C/min. As shown in Fig. 6, for a given PLLA/NAPAH sample,

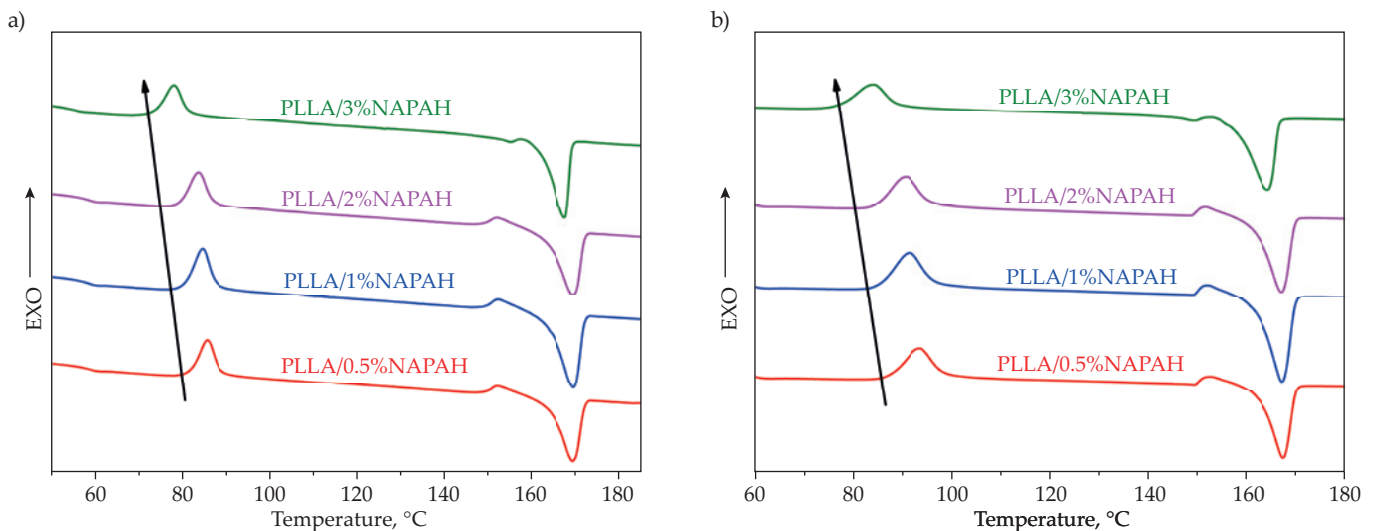


Fig. 5. Cold-crystallization of PLLA/NAPAH samples from the melt of 190°C at various heating rates: a) 1°C/min, b) 5°C/min

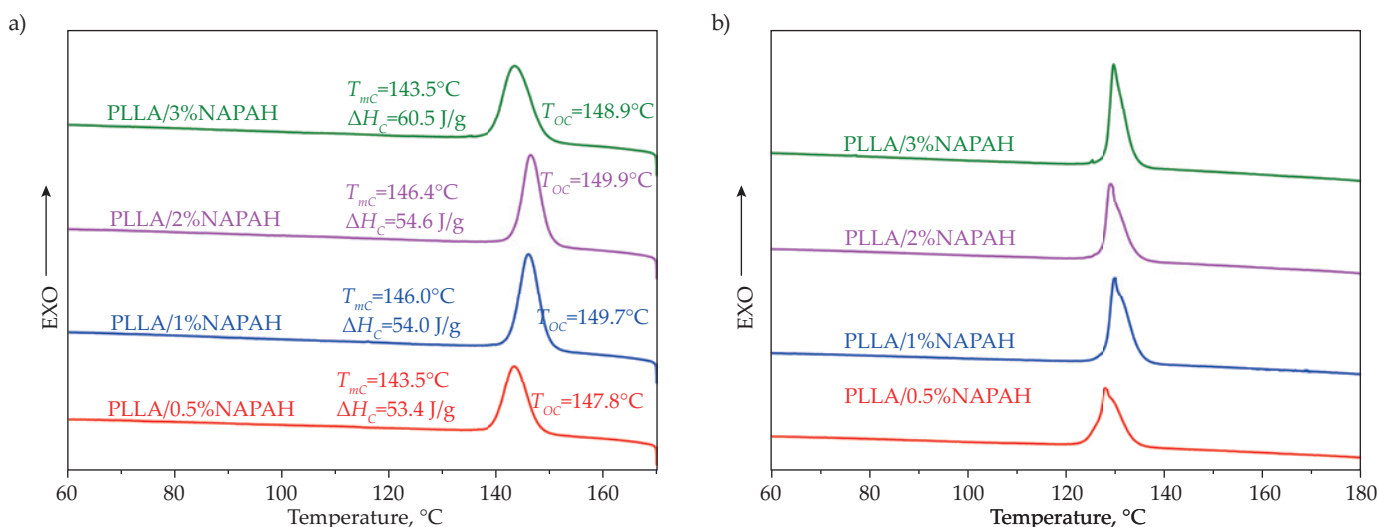


Fig. 6. Cooling processes of PLLA/NAPAH from different melt temperatures at 1°C/min coolingrate: a) 170°C, b) 200°C

the melt temperature of 170°C can induce the crystallization to start at the higher temperature compared with the other melt temperatures, and the T_{oc} and T_{mc} reach the maximum value, showing that the relative low melt temperature is beneficial for the crystallization of PLLA. In the presence of NAPAH, a relative low melt temperature can make the homogeneous nucleus of PLLA itself to form more rapidly in cooling because of the promoting effect of NAPAH for PLLA chain segment entanglement, ensuring a faster nucleation rate. However, a relatively low melt temperature is disadvantageous in crystal growth, which results in a wide crystallization peak, and except for PLLA/0.5%NAPAH, other PLLA/NAPAH samples have the largest ΔT . When the melt temperature is increased to 200°C, the T_{oc} and T_{mc} are decreased to the minimum value, but the PLLA with low NAPAH contents (0.5 wt% or 1 wt%) has the largest ΔH_c .

Melting behavior of PLLA/NAPAH

Usually, the melting process in second heating scan after crystallization must depend on the previous crystallization, whereas the previous crystallization is determined by the NAPAH and its content as reported by the crystallization behavior section. Thus, the difference in PLLA/NAPAH's melting behaviors can further address the role of NAPAH in matrix. Figure 7 shows the melting DSC curves of four PLLA/NAPAH samples after isothermal crystallization at different crystallization temperatures (T_c), the difference of T_c is 5°C in the temperature region of 110°C to 135°C, and they are 110, 115, 120, 125, 130 and 135°C, respectively. With increasing of T_c , the double melting peaks gradually fuse into a single melting peak, showing that the T_c is a crucial factor for crystallization, because a moderate T_c not only can cause crystal growth, but also won't destroy the formation of homogeneous nucleus. In the current melting process section, it is found that a relative high crystallization temperature

is beneficial for promoting PLLA's crystallization. In contrast, a low T_c cannot provide the fast crystal growth rate, resulting in the recrystallization occurring in heating, and the double melting peaks appear. Meanwhile, Fig. 7 also shows that the single melting peak is located at the higher temperature when increasing the T_c , what means that it is more difficult to melt crystals formed at higher T_c . Additionally, it is noted that PLLA/3%NAPAH has the lowest melting temperature among all PLLA/NAPAH samples. The probable reason is that a relatively large amount of NAPAH content added into PLLA, and the higher nucleation density in PLLA matrix lead to the crystal collision with their neighbors during the stage of crystal growth, thereafter, these less perfect crystals are melted in heating first, having the lower melting temperature. On the other hand, the existence of the excessive NAPAH is disadvantageous to the migration of PLLA chain segment, which results in the appearance of imperfect crystals.

As mentioned above, the cooling rate can significantly affect the crystallization process, and there is no doubt that the melting behavior depends on the cooling rate. Figure 8 shows the melting curves of PLLA/NAPAH at different heating rates (1, 2, 5°C/min) that corresponded to the rates of melt-crystallization at different cooling rates. Differing from the melt processes after isothermal crystallization, when PLLA/NAPAH is reheated to 180°C after melt-crystallization, the melting DSC curves of all PLLA/NAPAH have double melting peaks, showing that the recrystallization occurs again in heating. However, for a given PLLA/NAPAH, a slower cooling rate can make the low-temperature side melting peak appear at a higher temperature, suggesting that the crystals formed in cooling at a slower cooling rate are much more perfect. In addition, compared to the low-temperature side melting peak, the area of high-temperature side melting peak obviously becomes larger when the rate is increased; even when the rate is 5°C/min, the double melting peak area of PLLA/0.5%NAPAH is quite close.

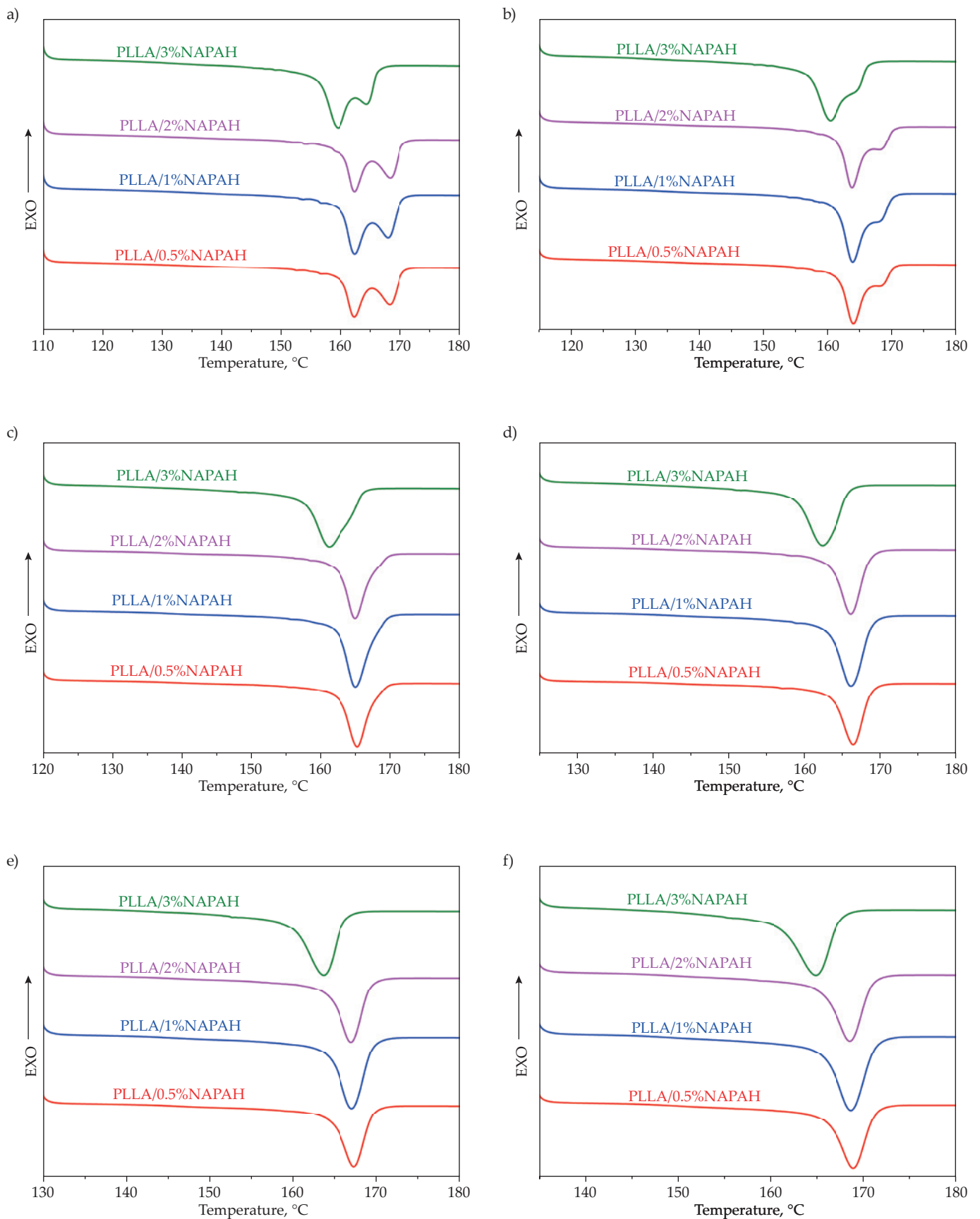


Fig. 7. Melting curves of PLLA/NAPAH after isothermal crystallization at different T_c and heating rate of 10°C/min: a) 110°C, b) 115°C, c) 120°C, d) 125°C, e) 130°C, and f) 135°C for 180 min

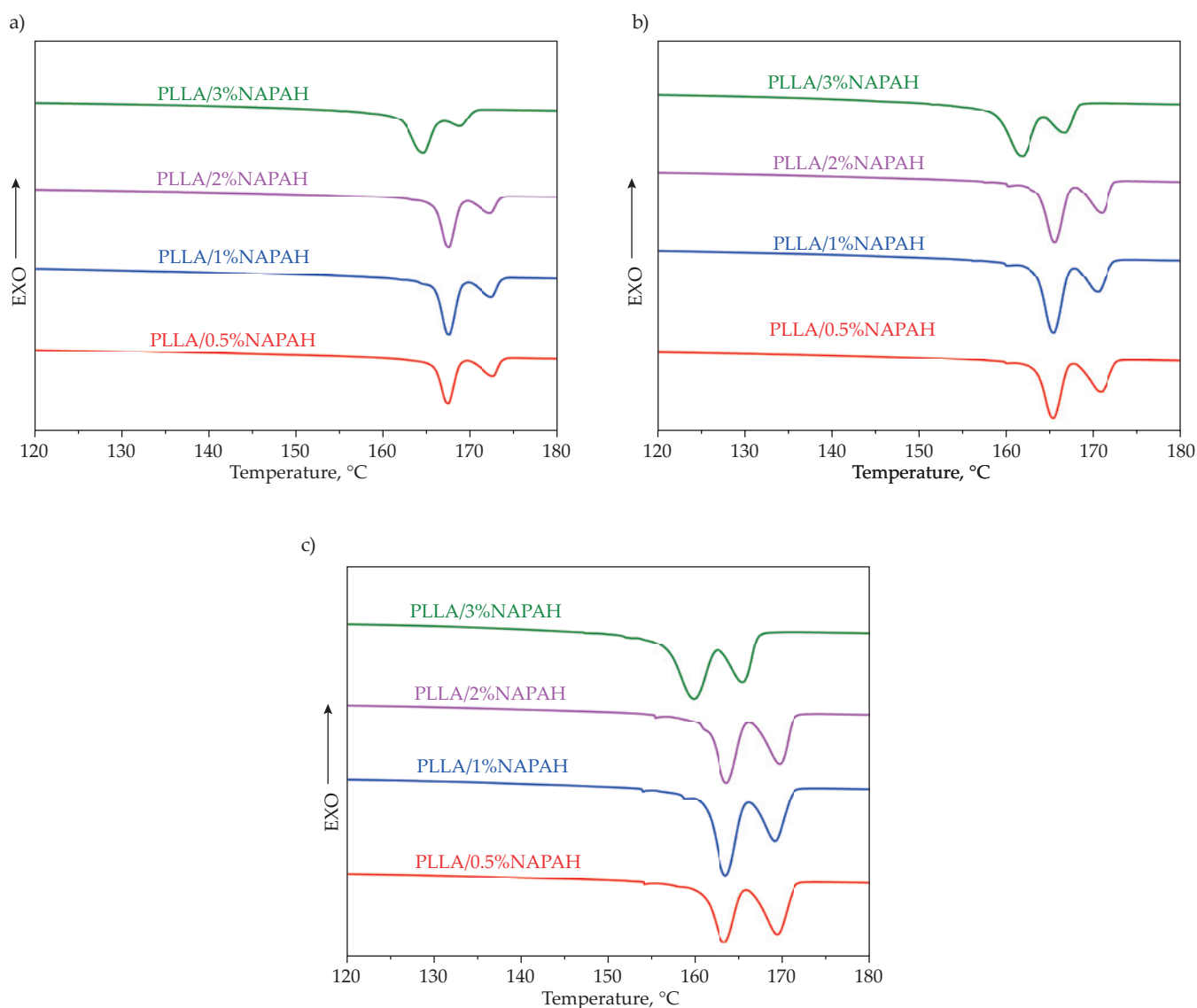


Fig. 8. Melting curves of PLLA/NAPAH after melt-crystallization at different heating / cooling rates: a) $-1^{\circ}\text{C}/\text{min} / 1^{\circ}\text{C}/\text{min}$, b) $2^{\circ}\text{C}/\text{min} / 2^{\circ}\text{C}/\text{min}$, c) $5^{\circ}\text{C}/\text{min} / 5^{\circ}\text{C}/\text{min}$

Thermal stability and processability of PLLA/NAPAH

Except for thermal deformation, the thermal decomposition is another important process to determine the critical point of polymer usage. Figure 9 shows thermal decomposition TGA curves of the virgin PLLA and PLLA/NAPAH in air. Differing from the thermal decomposition TGA curve of NAPAH (see Figure 2), Figure 9 clearly shows that all PLLA/NAPAH samples as the virgin PLLA have only one thermal decomposition stage in heating, and the decomposition temperature focuses on in the temperature region of 300°C to 400°C , which is consistent with the results reported by other works [6, 44, 45]. After completing aforementioned thermal decomposition, the weight-loss of all samples is almost up to 100%, meaning that the virgin PLLA and four PLLA/NAPAH samples are fully burned in heating. Under this circumstance, the study on thermal decomposition behavior

focuses more on the onset decomposition temperature (T_{od}). Through analysis of the T_{od} data obtained from TGA software, it is found that the T_{od} of any PLLA/NAPAH sample is lower than that of the virgin PLLA, and that the PLLA/1%NAPAH has the maximum T_{od} of 333.5°C , whereas the PLLA/3%NAPAH has the minimum T_{od} of 330.3°C . These results suggest that, on one hand, the existence of NAPAH in PLLA resin decreases PLLA's thermal stability; on the other hand, though that, upon heating at $5^{\circ}\text{C}/\text{min}$, the NAPAH has the lower T_{od} as seen in Fig. 1. T_{od} of PLLA/NAPAH cannot continuously decrease as NAPAH content increased, which indicates that a moderate NAPAH content (about 1 wt%) has the ability to prevent a drop in T_{od} . From the further analysis it is concluded that the probable interaction of C=O in PLLA with N-H in NAPAH improves the thermal stability of PLLA/NAPAH.

As it could be expected, the addition of NAPAH not only can improve the crystallization performance of PLLA, but also improves other performances. For actual

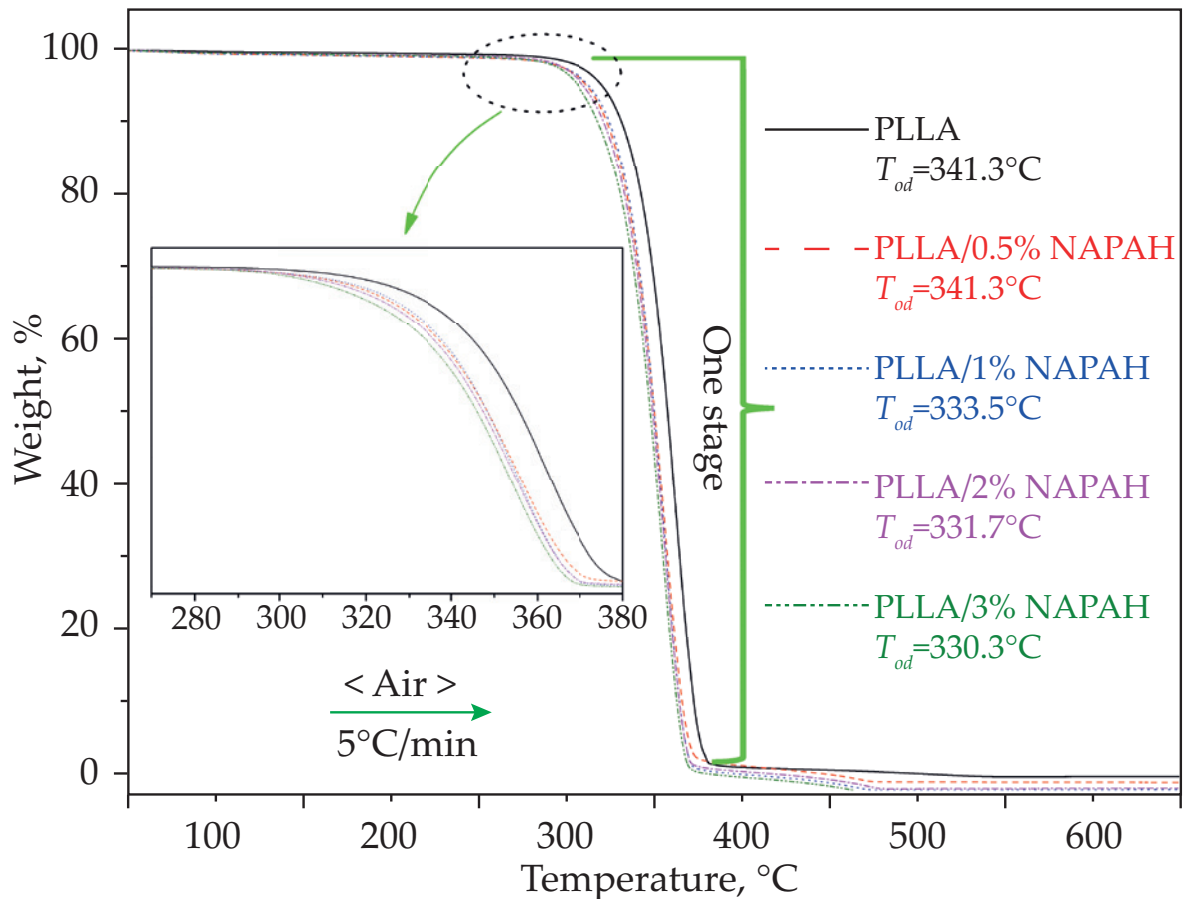


Fig. 9. TGA curves of the virgin PLLA and PLLA/NAPAH in air

manufacturing, the processability is related to the difficulty of injection molding. Herein, the effects of NAPAH and its content on the processability of PLLA were performed by a melt flow indexer (see Fig. 10), and the processability was characterized by melt flow rate (MFR) (A higher MFR often means the better processability). When the NAPAH content increases to 0.5 wt%, the MFR of PLLA/0.5%NAPAH is considerably enhanced up to, at least, 5 times with respect to the virgin PLLA, indicat-

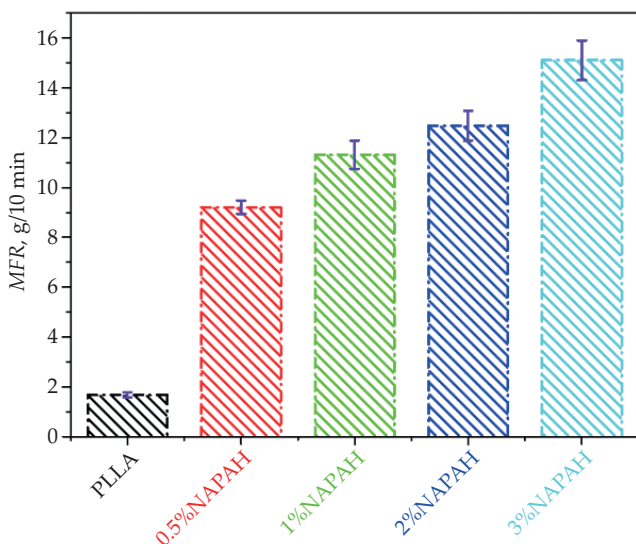


Fig. 10. MFR of the virgin PLLA and PLLA/NAPAH samples

ing that the NAPAH possesses the role in improving the processability of PLLA. However, when the NAPAH content increases from 0.5 wt% to 3 wt%, the MFR has only increased by 1.6 times, showing a slow upward trend. The reason is that a relative high NAPAH content has a bigger ability to aggregate during melt flow, which leads to an inhibition for the processability of PLLA chains by the physical barrier actions of aggregated NAPAH. However, on the other hand, the NAPAH itself can improve the processability of PLLA. As a result, the MFR is increased with increasing of NAPAH content in PLLA resin, but the increase is slowed down.

CONCLUSIONS

NAPAH was synthesized as an organic nucleating agent for PLLA, which showed excellent crystallization accelerating effect. By change of NAPAH content in PLLA matrix, cooling rate and melt temperature, the different melt-crystallization behaviors were observed. A larger amount of NAPAH possessed better crystallization ability, and upon cooling at 1°C/min from the melt of 190°C, the T_{oc} , T_{mc} and ΔH_c of PLLA/3%NAPAH could be up to 136.4°C, 132.4°C and 56.1 J/g, respectively. However, the increase in cooling rate and melting point was not favorable for PLLA crystallization in this work, and the addition of NAPAH to some extent inhibited PLLA cold crystal-

lization. The melting behavior after isothermal crystallization and melt-crystallization confirmed the crystallization promoting role of NAPA-H, and the crystallization temperature and heating rate significantly affected the melting behaviors, as well as the double melting peaks was thought to occur because of melting-recrystallization. The introduction of NAPA-H almost could not change the thermal decomposition profile of PLLA, because all PLLA/NAPA-H showed only one thermal decomposition stage in the virgin PLLA, but NAPA-H slightly decreased the thermal stability of PLLA, moreover, the existence of PLLA interaction with NAPA-H contributed to prevent the decrease of thermal stability. Apart from that, the addition of NAPA-H enhanced the processability of PLLA, and MFR of PLLA/NAPA-H was enhanced up to more than 5 times with respect to the virgin PLLA.

ACKNOWLEDGEMENTS

This study was supported by Chongqing Municipal Science and Technology Commission (cstc2019jcyj-msxmX0876), Scientific and Technological Research Program of Chongqing Municipal Education Commission (project number KJQN201801319) and Project of Chongqing University of Arts and Sciences.

REFERENCES

- [1] Ertas M., Altuntas E., Cavdar A.D.: *Polymer Composites* **2019**, 40(11), 4238.
<https://doi.org/10.1002/pc.25284>
- [2] Shuai C.J., Yuan X., Yang W.J. *et al.*: *Polymer Testing* **2020**, 85, 106450.
<https://doi.org/10.1016/j.polymer.2020.106458>
- [3] Bardot M., Schulz, M.D.: *Nanomaterials* **2020**, 10(12), 2567.
<https://doi.org/10.3390/nano10122567>
- [4] Zhen Z.Y., Xing Q., Li R.B. *et al.*: *Thermochimica Acta* **2020**, 683, 178447.
<https://doi.org/10.1016/j.tca.2019.178447>
- [5] Barczewski M., Mysiukiewicz O., Matykiewicz D. *et al.*: *Polymer Composites* **2020**, 41(7), 2947.
<https://doi.org/10.1002/pc.25589>
- [6] Huang A., Yu P., Jing X. *et al.*: *Journal of Macromolecular Science, Part B Physics* **2016**, 55(9), 908.
<https://doi.org/10.1080/00222348.2016.1217186>
- [7] Yan S.F., Yin J.B., Yang Y. *et al.*: *Polymer* **2007**, 48(6), 1688.
<https://doi.org/10.1016/j.polymer.2007.01.037>
- [8] Qiu S., Zhou Y.K., Waterhouse G.I.N. *et al.*: *Food Chemistry* **2021**, 334, 127487.
<https://doi.org/10.1016/j.foodchem.2020.127487>
- [9] Mohamad N., Mazlan M.M., Tawakkal I.S.M.A. *et al.*: *International Journal of Biological Macromolecules* **2020**, 163, 1451.
<https://doi.org/10.1016/j.ijbiomac.2020.07.209>
- [10] Mahmoodi A., Ghodrati S., Khorasani M.: *ACS Omega* **2019**, 4(12), 14947.
<https://doi.org/10.1021/acsomega.9b01731>
- [11] Han S.H., Cha M., Jin Y.Z. *et al.*: *Biomedical Materials* **2021**, 16(1), 015019.
<https://doi.org/10.1088/1748-605X/aba879>
- [12] Zhang H.Y., Jiang H.B., Kim J.E. *et al.*: *Journal of the Mechanical Behavior of Biomedical Materials* **2020**, 112, 104061.
<https://doi.org/10.1016/j.jmbbm.2020.104061>
- [13] Domalik-Pyzik P., Morawska-Chochol A., Chlopek J. *et al.*: *E-Polymers* **2016**, 16(5), 351.
<https://doi.org/10.1515/epoly-2016-0138>
- [14] Guzdemir O., Bermudez V., Kanhere S. *et al.*: *Polymer Engineering and Science* **2020**, 60(6), 1158.
<https://doi.org/10.1002/pen.25369>
- [15] Zhu F.C., Yu B., Su J.J. *et al.*: *Autex Research Journal* **2020**, 20(1), 24.
<https://doi.org/10.2478/aut-2019-0002>
- [16] Hammonds R.L., Gazzola W.H., Benson R.S. *et al.*: *Journal of Applied Polymer Science* **2014**, 131(15), 40593.
<https://doi.org/10.1002/app.40593>
- [17] Franca D.C., Almeida T.G., Abels G. *et al.*: *Journal of Nature Fibers* **2019**, 16(7), 933.
<https://doi.org/10.1080/15440478.2018.1441092>
- [18] Rychter P., Lewicka K., Rogacz D.: *Journal of Applied Polymer Science* **2019**, 136(33), 47856.
<https://doi.org/10.1002/app.47856>
- [19] Zawiska I., Siwek P.: *Folia Horticult Turae* **2014**, 26(2), 163.
<https://doi.org/10.1515/fhort-2015-0008>
- [20] Yan C., Jiang Y.P., Hou D.F. *et al.*: *Polymer* **2020**, 186: 122021.
<https://doi.org/10.1016/j.polymer.2019.122021>
- [21] Zhao C.X., Yu M.M., Fan Q.C. *et al.*: *Polymer for Advanced Technologies* **2020**, 31(5), 1077.
<https://doi.org/10.1002/pat.4842>
- [22] Cai Y.H., Yan S.F., Fan Y.Q. *et al.*: *Iranian Polymer Journal* **2012**, 21, 435.
<https://doi.org/10.1007/s13726-012-0046-x>
- [23] Li H.B., Huneault M.A.: *Polymer* **2007**, 48(23), 6855.
<https://doi.org/10.1016/j.polymer.2007.09.020>
- [24] Li X.X., Yin J.B., Yu Z.Y. *et al.*: *Polymer Composites* **2009**, 30, 1338.
<https://doi.org/10.1002/pc.20721>
- [25] Liao R.G., Yang B., Yu W. *et al.*: *Journal of Applied Polymer Science* **2007**, 104(1) 310.
<https://doi.org/10.1002/app.25733>
- [26] Su Z.Z., Guo W.H., Liu Y.J. *et al.*: *Polymer Bulletin* **2009**, 62(5), 629.
<https://doi.org/10.1007/s00289-009-0047-x>
- [27] Kawamoto N., Sakai A., Horikoshi T. *et al.*: *Journal of Applied Polymer Science* **2007**, 103(1), 198.
<https://doi.org/10.1002/app.25109>
- [28] Cai Y.H., Yan S.F., Yin J.B. *et al.*: *Journal of Applied Polymer Science* **2011**, 121(3), 1408.
<https://doi.org/10.1002/app.33633>
- [29] Roy M., Zhelezniakov M., de Kort G.W. *et al.*: *Polymer* **2020**, 202, 122680.

- <https://doi.org/10.1016/j.polymer.2020.122680>
- [30] Shen T.F., Xu Y.S., Cai X.X. *et al.*: *RSC Advances* **2016**, 6(54), 48365.
<https://doi.org/10.1039/c6ra04050k>
- [31] Xu X.K., Zhen W.J., Bian S.Z.: *Polymer-Plastics Technology and Engineering* **2018**, 57(18), 1858.
<https://doi.org/10.1080/03602559.2018.1434670>
- [32] Xu X.K., Zhen W.J.: *Polymer Bulletin* **2018**, 75(8), 3753.
<https://doi.org/10.1007/s00289-017-2233-6>
- [33] Huang H., Zhang Y.H., Zhao L.S. *et al.*: *Materiale Plastice* **2020**, 57(3), 28.
<https://doi.org/10.37358/MP.20.3.5377>
- [34] Zhao L.S., Cai Y.H.: *E-Polymers* **2020**, 20(1), 203.
<https://doi.org/10.1515/epoly-2020-0027>
- [35] Cai Y.H., Tang Y., Zhao L.S.: *Journal of Applied Polymer Science* **2015**, 132(32), 42402.
<https://doi.org/10.1002/app.42402>
- [36] Cai Y.H., Zhang Y.H., Zhao L.S.: *Journal of Polymer Research* **2015**, 22(12), 246.
<https://doi.org/10.1007/s10965-015-0887-z>
- [37] Cai Y.H., Zhao L.S.: *Polymer Bulletin* **2019**, 76(5), 2295.
<https://doi.org/10.1007/s00289-018-2498-4>
- [38] Su Z.Z., Li Q.Y., Liu Y.J.: *Polymer Engineering and Science* **2010**, 50, 1658.
<https://doi.org/10.1002/pen.21621>
- [39] Zhao L.S., Cai Y.H., Liu H.L.: *Polymer-Plastics Technology and Materials* **2020**, 59(2), 117.
<https://doi.org/10.1080/25740881.2019.1625386>
- [40] Borhan A., Taib R.M.: *Sains Malaysiana* **2020**, 49(9), 2169.
<https://doi.org/10.17576/jsm-2020-4909-15>
- [41] Somsunan R., Mainoiy N.: *Journal of Thermal Analysis and Calorimetry* **2020**, 139(3), 1941.
<https://doi.org/10.1007/s10973-019-08631-9>
- [42] Fan Y.Q., Zhu J., Yan S.F. *et al.*: *Polymer* **2015**, 67, 63.
<https://doi.org/10.1016/j.polymer.2015.04.062>
- [43] Kong W.L., Zhu B., Su F.M. *et al.*: *Polymer* **2019**, 168, 77.
<https://doi.org/10.1016/j.polymer.2019.02.019>
- [44] Behalek L., Boruvka M., Brdlik P. *et al.*: *Journal of Thermal Analysis and Calorimetry* **2020**, 142(2), 629.
<https://doi.org/10.1007/s10973-020-09894-3>
- [45] Xue B., He H.Z., Huang Z.X. *et al.*: *Journal of Applied Polymer Science* **2020**, 137(40), e49201.
<https://doi.org/10.1002/app.49201>

Received 13 VII 2022.

Rapid Communications

Przypominamy Autorom, że publikujemy artykuły typu **Rapid Communications** – **prace oryginalne wyłącznie w języku angielskim** (o objętości 4–5 stron maszynopisu z podwójną interlinią, zawierające 2–3 rysunki lub 1–2 tabele), którym umożliwiamy szybką ścieżkę druku (do 3 miesięcy od chwili ich otrzymania przez Redakcję). Artykuł należy przygotować wg wymagań redakcyjnych zamieszczonych we wskazówkach dla P.T. Autorów.

* * *

We remind Authors that we publish articles of the **Rapid Communications** type – **the original papers, in English only** (with a volume of 4–5 pages of double-spaced typescript, containing 2–3 figures or 1–2 tables), which allow a fast print path (up to 3 months from when they are received by the Editorial Board). The article should be prepared according to the editorial requirements included in the Guide for Authors.